small NANO MICRO

Biphasic morphology

DOI: 10.1002/smll.200600606

Phase Separation of Binary Blends in Polymer Nanoparticles

Thomas Kietzke, Dieter Neher, Michael Kumke, Omayma Ghazy, Ulrich Ziener, and Katharina Landfester**

***P**olymer blends in nanoparticles have been studied by transmission electron microscopy (TEM) and photoluminescence (PL) spectroscopy. The TEM studies show that blend particles formed from two immiscible polymers by the miniemulsion process exhibit biphasic morphologies. The fact that no core–shell type but Janus-like structures were found indicates that the surface free energies between both polymers and the solution–water interface (including the surfactant molecules) are similar; therefore, the blend morphology and composition of the individual phases are mainly determined by the interaction between the two polymer components. Both the TEM studies and the PL experiments provide strong evidence that phase separation in these particles strictly follows the Flory–Huggins theory. This highlights the applicability of the nanoparticle approach to fabricate blend systems with well-controllable properties and to study structure–property relationships under well-defined conditions.*

Keywords:
- emulsions
- nanoparticles
- phase separation
- polymer blends
- structure–property relationships

1. Introduction

The morphology of polymer blends and their relation to function has been a subject of ongoing research for many years. While earlier studies concerned the improvement of mechanical properties, the function–property relationship of polymer blends with electronic and optoelectronic properties has recently moved into focus.[1–3]

The phase properties of polymer blends can be well described theoretically by the Flory–Huggins theory. For binary blends of polymers A and B, the phase diagram (as a function of blend ratio) consists of two regions, related to the homogeneous blend and to the situation where the system phase-separates into two phases. Interestingly, the theory predicts that these phases are not pure and that the composition of each of these two phases depends only on temperature and not on the overall blend ratio. Evidently, the properties of phase-separated systems depend on the blend morphology (the length scale of phase separation) and also on the composition of the individual phases.

This is particularly important when considering thin layers of polymer blends, as used in functional optoelectronic organic devices such as polymer solar cells, field-effect transistors, and light-emitting diodes. The kinetics and efficiency of the elementary steps leading to these optoelectronic functions, which are, for example, the generation or recombination of charge carriers or the transfer of excitons, are highly influenced by the local environment of the active

[*] Dr. T. Kietzke, Prof. D. Neher
Institute of Physics, University of Potsdam
Am Neuen Palais 10, 14469 Potsdam (Germany)
Fax: (+49) 331-977-1083
E-mail: neher@uni-potsdam.de
O. Ghazy, Dr. U. Ziener, Prof. K. Landfester
Institute of Organic Chemistry
Macromolecular Chemistry and Organic Materials
University of Ulm
Albert-Einstein-Allee 11, 89069 Ulm (Germany)
Fax: (+49) 731-502-2883
E-mail: katharina.landfester@uni-ulm.de
Dr. T. Kietzke
Current address:
Institute of Materials Research and Engineering
3 Research Link, Singapore 117602 (Singapore)
Dr. M. Kumke
Institute of Chemistry, University of Potsdam
Karl-Liebknecht-Strasse 24–25, 14476 Golm (Germany)

sites. On the other hand, phase separation from a homogeneous mixture is a dynamic process and, consequently, the phase morphology is dependent on the sample history and on boundary conditions, as experimentally observed.[3] Thin multicomponent polymer layers are commonly deposited by spin-coating or printing techniques from a solution containing both polymers in the desired mass ratio. It is well documented that the surface properties of the substrate, the solvent from which the blend was deposited, the temperature, and certainly post-treatments largely influence the morphology of these thin layers.[2,4–6] This concerns the length scale of phase separation as well as the lateral and vertical composition of the phases.[7] Therefore, several recent studies have concerned the correlation between the nanomorphology and the local optical and optoelectronical properties of functional polymer-blend layers.[8–12] Dastoor and co-workers applied near-field scanning microscopy to correlate the local photocurrent with the layer morphology. They found that the photogeneration of current occurs primarily within the micron-sized phase-separated domains and not at the phase boundaries.[10] In a later study, the same authors published detailed investigations on the quantitative chemical composition of blends from two polyfluorenes.[11] As predicted by the Flory–Huggins theory, the phase-separated areas themselves consisted of a mixture of the two components, with a rather constant blend composition within the domains. In the same year, Cacialli and co-workers published a report on the correlation between the local fluorescence and photoconductivity and discussed their results with regard to the nanomorphologies of the layers.[12] Although these studies yielded interesting information on the morphology and the local optoelectronic properties of functional polymer blends, all measurements were performed on blend layers with lateral phase separation on the micrometer scale. However, many applications demand a nanoscale blend morphology. Also, the lateral resolution of the scanning-probe methods used in these studies is approximately 30–50 nm, which is well beyond the typical exciton diffusion length.

Recently, we presented a novel approach to control the length scale of phase separation of polymer blends on a length scale of a few tens of nanometers.[13] This approach involves the preparation of solid nanoparticles with well-controllable size through the formation of a miniemulsion of the polymer solution in water. Blends have been prepared in two ways, either by mixing nanoparticles of pure polymers (nanoparticle blend) or by forming blend nanoparticles by starting with a solution of both polymers. Spectroscopic investigations revealed that the latter approach leads to nanospheres containing both polymers in each particle and gave evidence for a phase-separated morphology. The incorporation of two polymers in a common solvent and application of the miniemulsion process is a novel approach to prepare nanoparticles including two or more polymers. It was further shown that the properties of optoelectronic devices fabricated from these particles are not related to the kind of solvent employed in the miniemulsion process, a fact indicating that the blend composition inside the nanoparticles is close to that at thermal equilibrium.

Here, we provide further information regarding the morphology of these blend particles. By using transmission electron microscopy, we demonstrate that the blend particles consist of two well-defined phases and that the respective volume fractions follow the well-known lever rule. The composition of the individual phases is acquired from spectroscopic studies on a blend of two fluorescent polymers. Finally, our results give strong evidence that the optical properties of these blends are largely determined by the composition of the individual phases and not by the blend morphology.

2. Results and Discussion

2.1. Microscopic Studies

Unfortunately, it was not possible to find a combination of polymers that allows the characterization of the same polymer-blend system with transmission electron microscopy (TEM) and optical spectroscopy. This is because the material contrast between different polymers in TEM is often low. Therefore, we decided to use a model system for the TEM measurement that allows the detailed characterization of the phase-separation processes in the particles. For these studies, polystyrene (PS; weight-average molecular weight $M_w = 101 \times 10^3\ g\,mol^{-1}$ (GPC, PS standard); glass temperature $T_g = 108\,^{\circ}C$ (DSC)) and poly(propylene carbonate) (PPC; $M_w = 39 \times 10^3\ g\,mol^{-1}$ (GPC, PS standard); $T_g = 16\,^{\circ}C$ (DSC)) were used since the two components can easily be distinguished in TEM measurements. In order to calibrate the experiments on the blend particles, micrographs were also taken from particles containing only one polymer component. For example, Figure 1 shows the TEM pictures of a blend of pure PS and PPC particles. The layer was prepared from a mixture of two aqueous particle dispersions of equal particle size (50 nm as determined by dynamic light scattering measurements) in a 1:1 ratio. Apparently, the contrast of both polymers in the TEM picture is very different: PS appears black and PPC is more "transparent" in the TEM image. The high density of hydrogen atoms in the structure of PPC with respect to the carbon background may explain the bright appearance of the PPC particles. Due to the low T_g value of PPC (16 °C), its particles probably melt under the conditions of TEM and do not show a well-defined morphology. We note that that the particles are statistically distributed and do not form separate domains.

Figure 2 shows TEM micrographs of PS:PPC blend particles of about 75 nm with different composition ratios. Evidently, all particles exhibit exactly two phases, separated by a rather flat interface. No evidence for a core–shell-type morphology is found, which would be expected if the preferable interaction between the surfactant molecules and one of the polymer components were the driving force for the phase-separation process. Volume fractions were calculated from the TEM images with the assumption of spherical particles occupied by each polymer in the particle. The calculated values (as listed in Table 1) are in good agreement with the values of the weight ratios of the polymers originally

small NANO MICRO

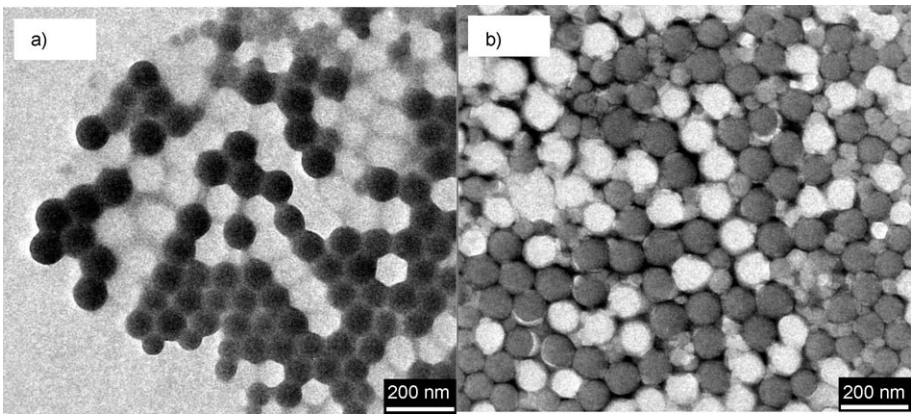

Figure 1. TEM images of a PS:PPC blend prepared by mixing two miniemulsions: a) without staining; b) negatively stained with uranium acetate.

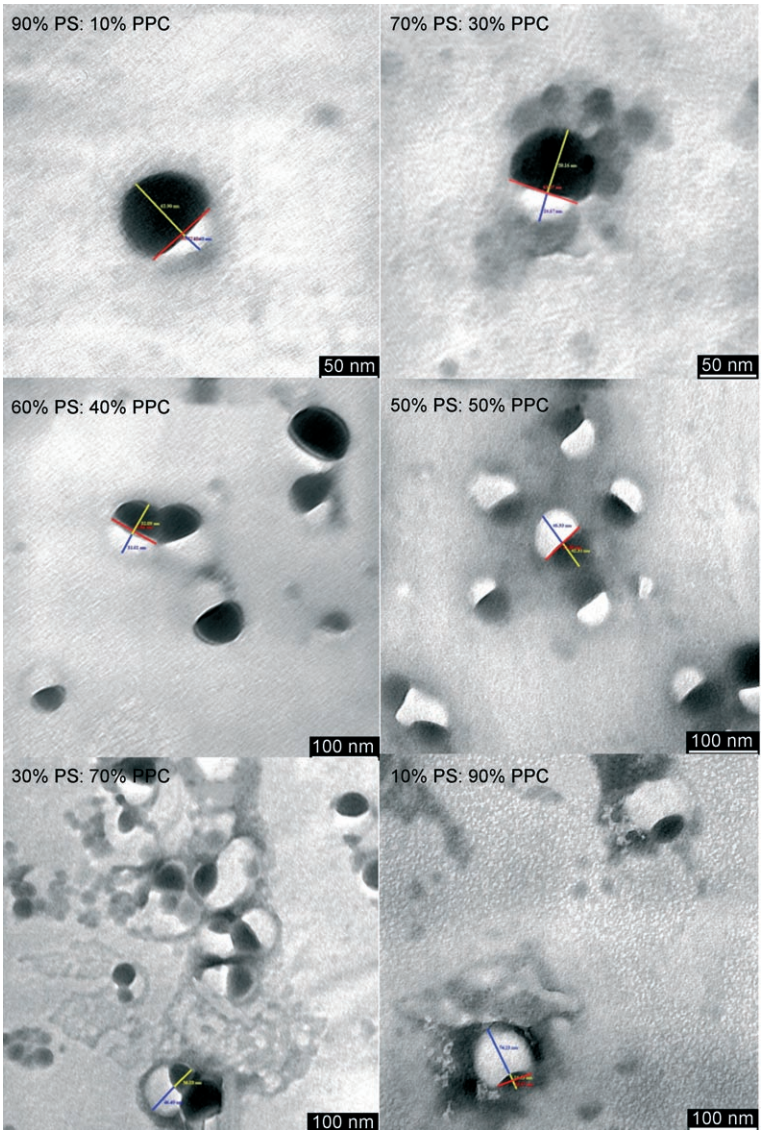

Figure 2. TEM images of different biphasic blend particles. (The percentages of the amounts employed in the preparation are given.) The particles are deposited on a carbon-coated copper grid and left to dry under air. The samples are not further labeled or stained.

used to prepare the nanoparticles. The percentage-wise relatively large deviation for the extreme compositions 90:10 and 10:90 can be explained by the fact that the assumption for the calculation of having a sphere and a sharp phase separation is not true and leads here to a larger error. The composition is not expected to be changed by the TEM preparation.

2.2. Spectroscopic Studies

It has been shown above that it is possible to prepare biphasic nanoparticles with the desired composition ratio and with well-defined morphology. In this section, we support this interpretation by studying the optical properties of nanoparticles formed by two emissive fluorene copolymers, poly(9,9-dioctylfluorene-2,7-diyl-*co*-bis-*N*,*N*'-(4-butylphenyl)-bis-*N*,*N*'-phenyl-1,4-phenylenediamine) (PFB) and poly(9,9-dioctylfluorene-2,7-diyl-*co*-benzothiadiazole) (F8BT). Since these two polymers are almost immiscible in each other, it can be assumed that blend particles of these two polymers exhibit the same morphology as the PS/PPC particles.

Blends of PFB and F8BT were chosen for several reasons: First, the main absorption and fluorescence lines of the two polymers are spectrally well separated, thereby allowing the excitation (and detection) of each individual component. Second, the photogenerated excitons can be dissociated between PFB, which accepts the hole, and F8BT, which accepts the electron. This process leads to quenching of the excitonic intrachain emission. Third, the PL spectrum of the blend

Table 1. Calculated volume percentage occupied by the two polymers in the nanoparticles for different weight ratios in the preparation.

PS:PPC polymer content[a]	Vol% of PS[b]	Vol% of PPC[b]
90:10	79	21
70:30	73	27
60:40	63	37
50:50	48	52
30:70	32	68
10:90	19	81

[a] Ratios measured in wt %, as used in the preparation of the nanoparticles. [b] As calculated from the TEM images of the nanoparticles.

exhibits emission from an interchain exciplex, which allows the study of the intermixing of the two components.[14,15] Finally, this system has been studied extensively with respect to photovoltaic properties and various correlations between photoresponse and blend morphology have been proposed.[2,4,5,7,14–16]

Figure 3 summarizes the relative PL efficiency and the normalized PL lifetime of each of the two polymers in blend particles for different blend ratios. The data have been taken from Ref. [17] and rearranged to highlight the correlation between PL quenching and PL-lifetime reduction. The relative PL intensities were obtained by normalizing the PL signal obtained for a certain F8BT fraction in the blend (ϕ_{F8BT}) to the emission of the respective pure component particles and dividing this number by the weight fraction of the emitting component in the blend. The values thus display the degree of quenching of, for example, the emission of PFB in the presence of F8BT (and vice versa). The normalized PL-lifetime data were obtained by dividing the values measured for the blend particles by the lifetime of the respective pure component particles.

There is a good correlation between the relative PL intensities and the PL lifetimes for both PFB and F8BT. Evidently, blending mainly causes additional nonradiative decay for the photogenerated excitons (through exciton dissociation) and leaves the radiative lifetime almost constant. As already discussed by us in our previous paper,[17] the emission properties are highly asymmetric with regard to blend composition. The PFB emission and lifetime is largely reduced upon addition of even small amounts of F8BT and is below the resolution limit of the PL detectors at a F8BT mass fraction of 0.33 (and above). By contrast, F8BT emission is clearly visible for all blend fractions. One particular point (not addressed in the original publication of these data) is that the F8BT emission lifetime is nearly constant over a rather broad range in composition ($\phi_{F8BT}=0.33$–0.83). This is in contrast to a naive picture where exciton split-up occurs mainly at the interface between the two phases and where the efficiency of quenching is determined by the probability that excitons generated in one of the two phases reach the interface.

In thermal equilibrium, the phase-separated blend should consist of a PFB-rich phase (A) and an F8BT-rich phase (B), with the respective mass fractions determined by

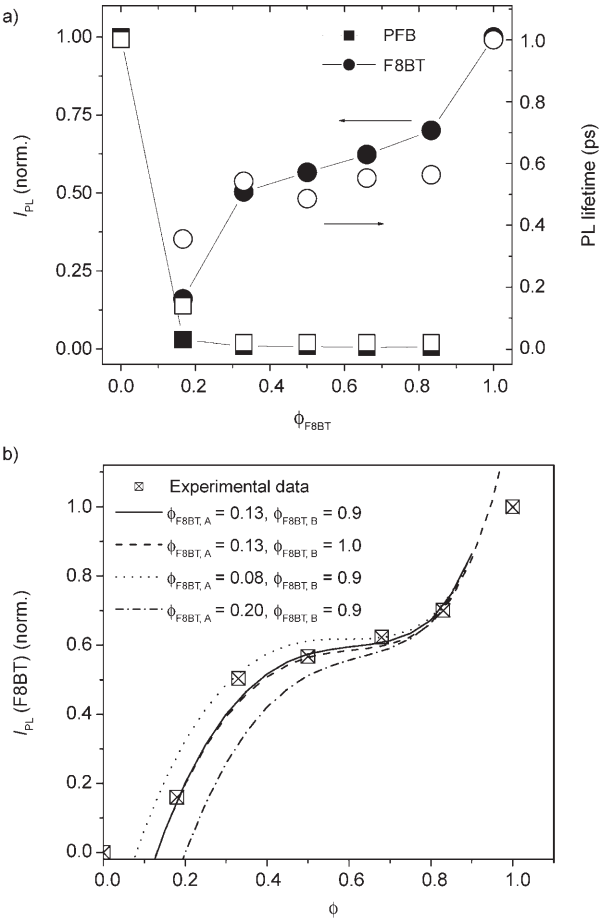

Figure 3. a) Relative PL intensities (solid symbols) and normalized PL lifetimes (open symbols) of the emission from PFB (squares) and F8BT (circles) measured on PFB:F8BT blend particles as a function of the F8BT content (data taken from Ref. [17]). PL intensities were measured in the steady state with excitation either at 380 nm (which excites mostly PFB) or 450 nm (which excites exclusively F8BT). PL lifetimes were recorded with an excitation wavelength of 394 nm. b) Prediction of the F8BT emission intensities under the assumption that only the F8BT-rich phase contributes to the PL signal and that the volume fraction of this phase is determined by the Flory–Huggins theory.

the lever rule [Eq. (1) and (2) with $m_A+m_B=1$].

$$m_A = \frac{\phi_{F8BT,B} - \phi_{F8BT}}{\phi_{F8BT,B} - \phi_{F8BT,A}} \quad (1)$$

$$m_B = \frac{\phi_{F8BT} - \phi_{F8BT,A}}{\phi_{F8BT,B} - \phi_{F8BT,A}} \quad (2)$$

Here, the relative mass fraction of F8BT in phase A with mass m_A is denoted by $\phi_{F8BT,A}$ and the F8BT mass fraction in phase B with mass m_B is denoted by $\phi_{F8BT,B}$, respectively. Within the two-phase region, the concentrations $\phi_{F8BT,A}$ and $\phi_{F8BT,B}$ are independent of ϕ_{F8BT}. As the relative F8BT emission decreases with a decrease in the ϕ_{F8BT} value (and thus an increase in m_A), it is plausible to assume that F8BT emission from the PFB-rich phase can be neglected. The almost

NANO MICRO small

complete absence of PFB emission for $\phi_{F8BT} > 0.2$ further suggests that all photoexcitations in phase A are completely quenched.

We could successfully model the relative F8BT intensity by assuming that the F8BT emission originates exclusively from phase B, as depicted in the schematic drawing in Figure 4. Figure 3b shows the results of calculations of the

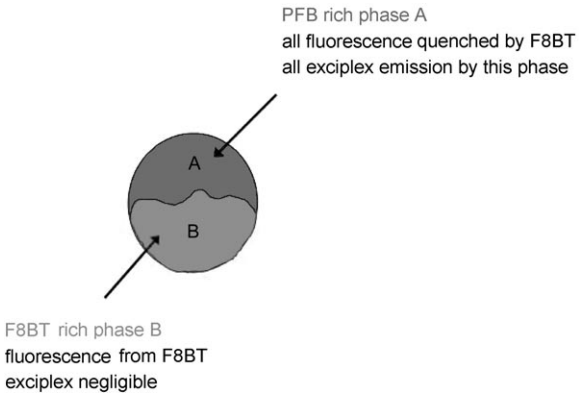

Figure 4. Schematic drawing of the phase separation inside a blend particle.

relative F8BT emission intensity. In these calculations, the mass fraction m_B was calculated from Equations (1) and (2) for different values of $\phi_{F8BT,A}$ and $\phi_{F8BT,B}$. Also, the PL quantum efficiency η_{F8BT} was assumed to be strictly linear with the PL lifetime. As shown in Figure 3b, the comparison of the calculated and the measured values sets tight limits for the compositions of the two phases. Best fits were obtained with a concentration of F8BT in the PFB-rich phase of 0.13–0.15, while the F8BT concentration in the F8BT-rich phase should be above 0.9. Apparently, both phases contain small minority components of the respective second component.

To verify these estimates, we have further considered the exciplex contribution to the emission in thin blend layers. Exciplex emission in PFB:F8BT blends was first reported by Morteani et al.[15] As it requires the PFB and F8BT chains to be in close proximity, the relative strength of exciplex emission is a good measure for the degree of polymer intermixing. Figure 5a shows emission spectra of blends spin-coated from chloroform and xylene as well as of nanoparticles prepared with either of the two solvents. The exciplex emission is clearly seen as a peak with a maximum at approximately 615 nm for the film spin-coated directly from chloroform and appears as a weak shoulder for the layer coated from xylene. Chloroform evaporates much faster than xylene and leaves the polymers less time to approach their thermodynamic equilibrium during drying of the spin-coated layer. As a result, the phase separation in films prepared from chloroform is on a much smaller scale than that for the xylene case,[2] thereby leading to a higher overall interfacial area between the polymers and thus more exciplexes being formed. By contrast, the different solvents used for the initial preparation of the nanoparticles have only a weak effect on the PL, which indicates that the

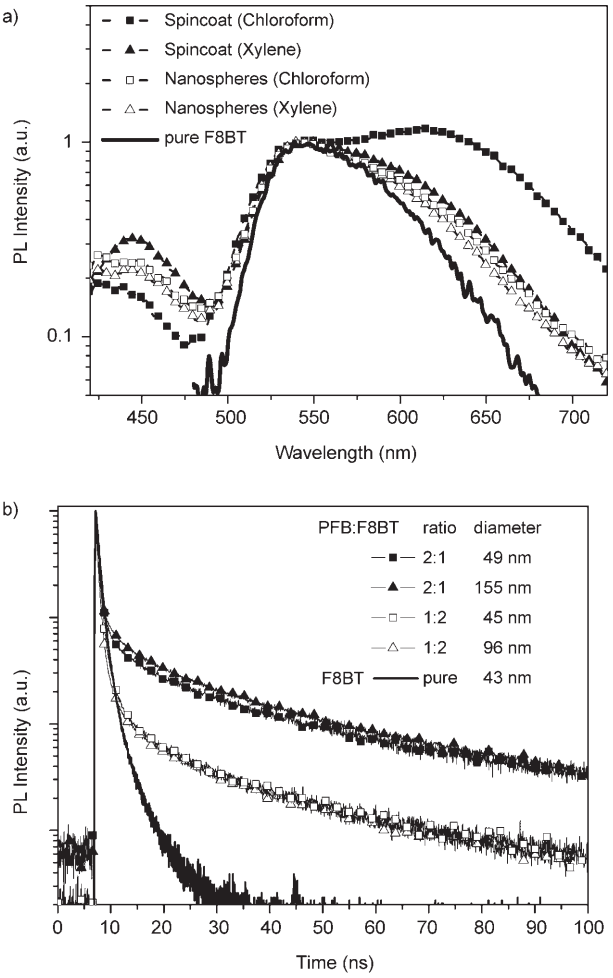

Figure 5. a) Steady-state PL emission spectrum (excitation wavelength = 380 nm) of blend layers coated from chloroform and xylene and of monolayers of 1:1 blend particles. Particle formation involved 1:1 solutions of the polymers in either chloroform or xylene. b) Transient PL spectrum for PFB:F8BT blend particles with two different blend ratios and two different particle sizes. The excitation wavelength was 392 nm and the detection wavelength was 625 nm.

phases formed in the nanoparticles are closer to the thermal equilibrium. The exciplex contribution becomes more noticeable when the results from time-resolved PL emission studies are considered, as shown in Figure 5b. The exciplex contribution leads to a slowly decaying component, with an average lifetime of 100 ns. Evidently, the decay characteristic is largely determined by the blend ratio while the actual particle size is of minor importance. This suggests that exciplex formation takes place mainly between dissimilar chains within the individual components and not at the interface between different phases. A second observation is that the relative exciplex contribution decays largely with increasing F8BT concentration. This leads to the conclusion that most exciplex emission is generated in the PFB-rich phase (Figure 5).

In order to quantify this, we have deconvoluted the steady-state emission spectra for excitation at 380 nm and 460 nm. The exciplex emission intensity was then divided by

the total absorbance at the respective wavelength. As the exciplex contribution decays with increasing F8BT content, it was assumed that exciplex emission originates only from the PFB-rich phase and that the quantum efficiency for exciplex formation is independent of the overall blend composition. Figure 6 shows the normalized exciplex emission intensities for excitation at 380 (mainly PFB) and 460 nm (only F8BT). Also shown are the results of calculations based on the Flory–Huggins theory as outlined above. The calculated dependence of the exciplex emission on the particle composition turned out to be rather insensitive to the concentration of F8BT in the PFB-rich phase but very sensitive to its concentrations in the F8BT-rich domains.Very good agreement between the calculated and the experimental values is found for $\phi_{F8BT,B} = 0.9$–0.95.

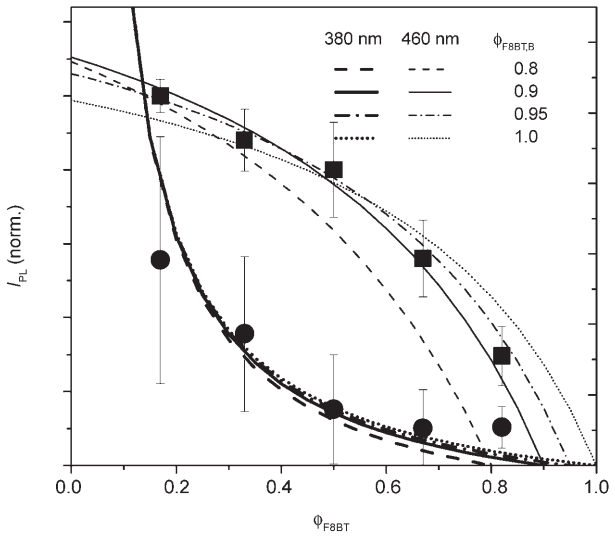

Figure 6. The steady-state PL intensity at 625 nm of the PFB:F8BT blend particles for an excitation wavelength of 380 nm (squares) and 460 nm (circles). Data were obtained by subtracting the pure emission contributions from PFB and F8BT and by normalizing these values to the absorbance at the respective excitation wavelengths. The measured values (solid symbols) are compared with predictions from the Flory–Huggins theory (lines) under the assumption that the exciplex emission stems exclusively from the PFB-rich phase. In all calculations, the concentration of F8BT in the PFB-rich phase was 0.13.

3. Discussion and Conclusions

Our TEM studies prove unambiguously that blend particles formed from two immiscible polymers through the miniemulsion process exhibit biphasic morphologies. The fact that no core–shell-type but Janus-like structures were found indicates that the interaction between the solution–water interface (including the surfactant molecules) and each of the polymer phases is similar and that there is no preference of one polymer to the water phase. At this point, we note that the kinetics and structure of phase separation in polymer-blend particles has been studied earlier by others.[18–24] Although these particles were mostly fabricated from emulsions of dilute polymer solutions, as for the particles reported here, the average particle sizes in those studies ranged between several hundreds of nanometers to a few micrometers. Also, those reports were exclusively on nonconjugated polymers. To the best of our knowledge, our paper contains the first detailed report on the morphology of phase separation in true nanoparticles of functional polymers. Our TEM studies and the PL experiments provide strong evidence that phase separation in these particles strictly follows the Flory–Huggins theory. This highlights the applicability of the nanoparticle approach either to fabricate blend systems with well-controllable properties or to study structure–property relationships under well-defined conditions.

For the PFB–F8BT blend, our studies show that the PFB-rich phase contains F8BT at a concentration of approximately 15%, while the concentration of PFB in the F8BT-rich phase is even smaller, probably between 5–10%. The larger concentration of F8BT in the PFB-rich phase (as compared to the concentration of PFB in the F8BT-rich phase) is understandable with consideration of the significantly larger molecular weight of PFB. According to the Flory–Huggins theory, the pronounced asymmetry in phase composition when blending two polymers with unequal molecular weights is due to the fact that only the diffusion of short polymer chains into the phase with predominant long chains leads to a substantial increase in entropy. Therefore, the phase rich in the short-chain component (F8BT in this case) should contain only a small fraction of the long-chain polymer (PFB). In fact, the phase composition found in this study is quite consistent with the prediction of the Flory–Huggins theory for $\chi N_1 = 1.4$–1.6 (with χ being the Flory–Huggins interaction parameter and N_1 being the degree of polymerization of the shorter chain polymer).

As mentioned earlier, McNeill et al. recently mapped the chemical composition of polymer-blend layers based on F8BT and poly(9,9-dioctylfluorene-co-*N*-(4-butylphenyl)diphenylamine (TFB) with approximately 50 nm lateral resolution.[11] These layers had been coated with *p*-xylene to induce lateral phase separation at the micrometer scale. The authors found a concentration of TFB in the TFB-rich domains of approximately 68–76 wt%. The F8BT concentration in the F8BT-rich domains was approximately 90 wt% near the interface to the TFB-rich domain and approximately 60 wt% away from this interface. These findings suggest a rather high degree of mixing within the phases, which is particularly surprising when the very high molecular weights of the used polymers ($M_w = 119\,000\ g\,mol^{-1}$ and $151\,000\ g\,mol^{-1}$ for TFB and F8BT, respectively) are considered. Presumably, the phase-separation process in these spin-coated layers is not yet complete and the morphology is frozen at a nonequilibrium state during evaporation of the solvent.

Our studies indicate that the optical properties of the PFB:F8BT blend systems are mainly determined by the composition of the individual phases and not by the phase morphology: the PL results as a function of blend composition can be well explained if one assumes that the F8BT luminescence originates predominantly from the F8BT rich

NANO MICRO small

phase while the exciplex emission stems from the PFB rich phase (Figure 4). This result is quite surprising if the small length scale of phase separation in these particles (as defined by the particle diameter) is kept in mind. Apparently, the minority components in the individual phases largely reduce the exciton diffusion length and most excitons decay or dissociate within the domains rather than at the domain boundaries. As both exciplexes and free charge carriers have the same precursor state, namely a dark geminate pair,[14] our findings further imply that carrier photogeneration mainly occurs within the PFB-rich domains. This conclusion is in very good agreement with the results of AFM and near-field scanning photocurrent microscopy studies on blend layers of PFB and F8BT published by Dastoor and co-workers, as mentioned earlier.[10] Interestingly, Cacialli and co-workers recently concluded that the photocurrent originates mainly from the protruding F8BT-rich areas.[12] This contrariety of results, measured by two different groups on different samples, shows that the optoelectronic response in polymer blend systems depends largely on the local composition and morphology, which is not well controllable in spin-coated layers. Apparently, there is a need for the intensive study of well-defined polymer–polymer blends. The nanoparticles investigated in this paper might serve as ideal model systems to establish structure–function relationships in nanoscale phase-separated blends.

4. Experimental Section

Synthesis of the aqueous polymer dispersions: For the PS and PPC dispersions, the polymer (mixture; 50 mg) was dissolved in $CHCl_3$ (5 g) and added to an aqueous solution comprising sodium dodecyl sulfate (SDS; 30 mg) and water (10 g). PFB ($M_w = 100\,000\ g\,mol^{-1}$) and F8BT ($M_w \approx 20\,000\ g\,mol^{-1}$) were purchased from American Dye Sources. For the preparation of the dispersions, single-polymer solutions in chloroform or solutions of the two polymers in chloroform (at 2.5 wt%) were added to an aqueous SDS solution (100 mg SDS/10 g water).

After 15 min of stirring for pre-emulsification, the miniemulsion was prepared by sonicating the mixture for 3 min at 65% amplitude (Branson sonifier W450). The samples were left stirring for 2 h at 60 °C to evaporate the chloroform from the liquid droplets in order to obtain an aqueous dispersion. To eliminate the excess surfactant and concentrate the samples, the dispersions were dialyzed against demineralized water by using a Millipore membrane (Amicon Ultra −4; exclusion M_w of 30 000) in a Sigma centrifuge at 2500 rpm, until the conductivity of the water was about 10 $\mu S\,cm^{-1}$. The final dispersions had 7% solid content and 5% SDS to the amount of polymer. The particles sizes were measured by using a Nicomp particle sizer at a fixed scattering angle of 90°.

Optical spectroscopy: Absorption spectra were recorded with a Perkin–Elmer Lambda 19 UV/Vis spectrometer. The spectra were corrected for the transmission of the uncoated glass slides in the case of film measurements and for the transmission of the cuvettes in the case of dispersions measurements.

Steady-state fluorescence spectra were measured with a Perkin–Elmer LS 50 luminescence spectrometer. The excitation was incident at an incident angle of 60° onto the front face of the sample and the emission was recorded in reflection at an angle of 30°.

Details about the fluorescence lifetime measurements can be found in Ref. [17]. In short, the highly diluted dispersions were excited with a mode-locked Ti:sapphire laser (Tsunami, Spectra Physics) after second-harmonic generation at $\lambda_{ex} =$ 392 nm and the fluorescence of the samples was detected by a streak camera (C5680, Hamamatsu) equipped with an imaging spectrograph (250is, Chromex).

Fluorescence decay measurements on a longer timescale (0.1–100 ns) were performed with an FL920 fluorometer (Edinburgh Instruments, Livingston, UK). Fluorescence decays were measured with a multichannel plate (ELDY EM1–132 300 MCP-PMT, Europhoton, Berlin). The complete detection system had an instrumental response time of 100 ps. For data analysis, the commercial software package provided with the FL920 fluorescence spectrometer was used. The experimental fluorescence decay data were iteratively deconvolved from the instrument response function based on a Marquardt algorithm.

Acknowledgements

We would like to thank Prof. Dr. H.-G. Löhmannsröben and Dr. W. Regenstein (University of Potsdam) for access to the optical spectrometers used in this work. We also acknowledge financial support by the Stiftung Volkswagenwerk and the Fonds der chemischen Industrie (FCI).

[1] Y. Kim, S. Cook, S. A. Choilis, J. Nelson, J. R. Durrant, D. D. C. Bradley, *Chem. Mater.* **2004**, *16*, 4812.
[2] A. C. Arias, J. D. MacKenzie, R. Stevenson, J. J. M. Halls, M. Inbasekaran, E. P. Woo, D. Richards, R. H. Friend, *Macromolecules* **2001**, *34*, 6005.
[3] Y. Xia, R. H. Friend, *Macromolecules* **2005**, *38*, 6466.
[4] C. M. Ramsdale, J. A. Barker, A. C. Arias, J. D. MacKenzie, R. H. Friend, N. C. Greenham, *J. Appl. Phys.* **2002**, *92*, 4266.
[5] H. J. Snaith, A. C. Arias, A. C. Morteani, C. Silva, R. H. Friend, *Nano Lett.* **2002**, *2*, 1353.
[6] R. Stevenson, A. C. Arias, C. Ramsdale, J. D. MacKenzie, D. Richards, *Appl. Phys. Lett.* **2001**, *79*, 2178.
[7] A. C. Arias, N. Corcoran, M. Banach, R. H. Friend, J. D. MacKenzie, *Appl. Phys. Lett.* **2002**, 80, 1695.
[8] J. Chappell, D. G. Lidzey, P. C. Jukes, A. M. Higgings, R. L. Thompson, S. O'Connor, I. Grizzi, R. Fletcher, J. O'Brien, M. Geoghegan, R. A. Jones, *Nat. Mater.* **2003**, *2*, 616.
[9] A. Cadby, R. Dean, R. A. L. Jones, R. G. Lidzey, *Adv. Mater.* **2006**, *18*, 2713.
[10] C. R. McNeill, H. Frohne, J. L. Holdsworth, P. C. Dastoor, *Nano Lett.* **2004**, *4*, 2503.
[11] C. R. McNeill, B. Watts, L. Thomsen, W. J. Belcher, N. C. Greenham, P. C. Dastoor, *Nano Lett.* **2006**, *6*, 1202.
[12] R. Riehn, R. Stevenson, D. Richards, D.-J. Kang, M. Blamire, A. Downes, F. Cacialli, *Adv. Funct. Mater.* **2006**, *16*, 469.
[13] T. Kietzke, D. Neher, K. Landfester, M. Montenegro, R. Güntner, U. Scherf, *Nat. Mater.* **2003**, *2*, 408.

[14] A. C. Morteani, P. Sreearunothai, L. M. Herz, R. H. Friend, C. Silva, *Phys. Rev. Lett.* **2004**, *92*, 247 402.
[15] A. C. Morteani, A. S. Dhoot, J.-S. Kim, C. Silva, N. C. Greenham, C. Murphy, E. Moons, S. Cina, H. Burroughes, R. H. Friend, *Adv. Mater.* **2003**, *15*, 1708.
[16] J. A. Barker, C. M. Ramsdale, N. C. Greenham, *Phys. Rev. B* **2003**, 67, 075 205.
[17] T. Kietzke, D. Neher, M. Kumke, M. Montenegro, K. Landfester, U. Scherf, *Macromolecules* **2004**, *37*, 4882.
[18] C. L. Winzor, D. C. Sundberg, *Polymer* **1992**, *33*, 4269.
[19] Y.-C. Chen, V. Dimonie, M. S. El-Aasser, *J. Appl. Polym. Sci.* **1992**, *46*, 691.
[20] Y. C. Chen, V. L. Dimonie, O. L. Shaffer, M. S. El-Aasser, *Polym. Internat.* **1993**, *30*, 185.
[21] G. H. Ma, M. Nagai, S. Omi, *J. Colloid Interface Sci.* **1999**, *214*, 264.
[22] M. D. Barnes, K. C. Ng, K. Fukui, B. G. Sumpter, D. W. Noid, *Macromolecules* **1999**, *32*, 7183.
[23] D. C. Sundberg, Y. G. Durrant, *Polym. React. Eng.* **2003**, *11*, 379.
[24] J. M. Stubbs, Y. G. Durant, D. C. Sundberg, *Compt. Rend. Chimie* **2003**, *6*, 1217.

Received: October 31, 2006
Revised: February 7, 2007
Published online on May 7, 2007

